Nov 6th, 12:00 AM - 12:00 AM

Study on the Flexural Capacity of Cold-Formed Steel Joists-OSB Composite floors

X. H. Zhou

Y. Shi

R. C. Wang

Y. J. Liu

Twenty-Second International Specialty Conference on Cold-Formed Steel Structures
St. Louis, Missouri, USA, November 5 & 6, 2014

Study on the flexural capacity of cold-formed steel joists-OSB composite floors

X.H. Zhou [1], Y.Shi [2], R.C.Wang [3], Y.J. Liu [4]

Abstract: Two full scale specimens were tested to study the flexural capacity of cold-formed steel joists and OSB(Oriented strand board) composite floors. Test results indicated the composite floors had high bearing capacity and small deformation, and the screw spacing significantly affected the load-carrying capacity. The main failure modes were flexural and torsional buckling of floor joist, and the interactive buckling of compression flange, web and crimp. The wave length of bucking equalled to the adjacent screw spacing. Then the specimens were analyzed by commercial software ANSYS and the nonlinear FEM calculation results agreed well with the test results. Furthermore, detailed research on the influence of the screw spacing and the length-width ratio was carried out in order to understand the factors affecting the flexural capacity of the composite floors. FEM analysis results indicated that the reasonable screw center spacing is 150mm at OSB edges and 150~300mm at intermediate supports. Also the load-carrying capacity of the composite floors linearly increased along with the decrease of the joist spacing. Finally, a simplified calculation model and method were proposed on the basis of experimental study and FEM analysis.

[1]Professor, Academician of Chinese Academy of Engineering, College of Civil Engineering, Chongqing University, Chongqing, 400045, China, <zhouxuhong@126.com>
[2] Associate Professor, School of Civil Engineering, Chang'an University, Xi'an, Shannxi, 710061, China, <shiyu7811@163.com>
[3] Engineer, Shanxi Electric Power Exploration & Design Institute, Taiyuan, Shanxi, 703000, China, <185911763@qq.com>
[4] Professor, School of Highway, Chang'an University, Xi'an, Shannxi, 710064, China<steellyj@126.com >

1. Introduction

Cold-formed steel structures have been widely used for commercial and residential buildings. Floor system built with cold-formed steel joists and oriented strand board(OSB) sheathing(NASFA, 2000), is one of the main bearing components of cold-formed steel structures. The OSB sheathing serves the primary function of providing lateral restriction for cold-formed steel joists and transmitting loads into the structures.

Nader R.(1999) investigated the horizontal diaphragm experiments of cold-formed steel joists-OSB composite floor in order to test its stiffness and ultimate shear strength. Afterwards, extensive studies focused on the dynamic response and stiffness of cold-formed steel joists-OSB composite floor system were carried out by Xu L.(2007, 2011) through both laboratory work and in situ conditions. Teng X.F.(2009)and Zhou X.H.(2010, 2013) studied the flexural capacity of cold-formed steel floor by means of full scale model tests. Previous research suggested that interaction between floor panel and joists has some effects on the bearing capacity of floor. Nevertheless, when defining the flexural bearing capacity of cold-formed steel composite floor, China design code (GB 50018, 2002) only considers the function of cold-formed steel joists but ignores the combined contribution of floor panel and joists.

This paper puts forward a simplified calculation model and method to calculate the flexural capacity of cold-formed steel joists-OSB composite floors with consideration of combined action of floor panel and joists, based on the two full-scale floor system experiments undertaken at Chang'an University(Zhou X.H., 2013) and a detailed finite element analysis.

2. Experimental Investigation

2.1 Laboratory Specimen Details

The purpose of the laboratory investigation is to test the flexural bearing capacity of cold-formed steel joists-OSB composite floor(Zhou X.H., 2013).The detailed structural diagrams of specimen FL-1 was shown in Figure 1, each specimen was 2.4m wide by 4.8m long (Figure 1(a)). The floor specimen consisted of seven 4.8m-long cold-formed steel joists spacing 400mm and 18mm OSB sheathing. The steel skeleton was constructed with C-shape C305mm×41mm×14mm×1.6mm joists and U-shape U305mm×35mm×1.6mm

tracks(Figure 1(b)). The joist ends were connected to the cold-formed steel rim-tracks by ST4.8 headed self-drilling self-tapping screws, and the distance of screw center to the edge of joist was 20mm. A web bearing stiffener was fastened to each end of joist with nine ST4.8 self-drilling self-tapping screws as shown in Figure 1(c) in order to avoid web crippling at bearing locations. The bearing stiffener was with the same cross-section as the floor joist, and with length less than 50mm of the web height of joist. The OSB sheathing was fastened to the joists using ST4.8 self-drilling screws. The only difference between the specimen FL-1 and specimen FL-2 was the screws spacing between the OSB sheathing and steel skeleton. In the specimen FL-1, OSB sheathing was fastened to the cold-formed steel skeleton with 150mm center spacing around the perimeter of OSB sheathing, and 300mm inside the panel. At the same time, the sheathing screws were arranged with 300mm center distance at panel edges and 600mm at intermediate supports in the specimen FL-2. All screws protruded through steel framing members with a minimum of three exposed threads.

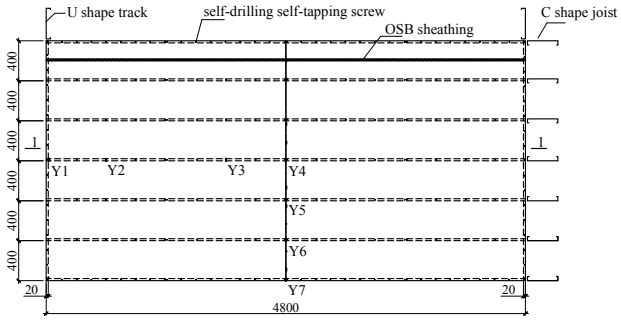

(a)layout of specimen FL-1

(b) Steel skeleton of specimen FL-1

(c) bearing stiffener

Figure 1 Basic construction specimen FL-1

The mechanical properties of the cold-formed steel used in the specimens were obtained by standard tensile coupon tests(GB/T 228.1, 2010). Three coupons were cut from the web of cold-formed steel joist. The average uncoated steel thickness was 1.56mm.The average yield strength and tensile strength of steel

were 334.04N/mm^2 and 447.73N/mm^2 respectively; the average elongation rate after fracture was 32.80%; the elastic modulus was 2.08×10^5 N/mm^2; and the average Poisson's ration was 0.3.

2.2 Test setup and measuring point layout

As shown in Figure 2, the tested floor system was supported along the two U-shape tracks by a heavy steel frame mounted to concrete ground beams. A 3m-length L-shape angle-steel L50×5 was welded on the heavy steel beamof steel frame to support the ends of the floor system. The tested floor system was loaded using a hydraulic cylinder and four spreader beams to simulate uniformly distributed load. Ten percent of the estimated design load was applied to each load step. Each increment was held for ten minutes after which loads and deflections were recorded. All the data were automatically collected by a TDS-602 data acquisition system.

Figure 2 Floor test apparatus

The displacement sensors were arranged in Figure 1 to measure the specimen's deflection. Considering the symmetry of the floor system, the displacement meters Y1 ~ Y4 were used to measure the floor deflection along the middle joist. Y1 was arranged at bearing support, Y2 and Y3 were arranged at the location of spreader beam, and Y4 was located at min-span of the joist. The displacement meters Y5~Y7 were arranged to measure the maximum deflection of joists to observe the deflection trend from the center to the edge.

2.3 Test Results

Actual load-deflection curves measured from the tests were shown in Figure 3; the deflection was the data of displacement meter Y4 subtracted the value of displacement meter Y1. The flexural bearing capacity was collected in Table 2. In the tests, both tested floor systems failed when the cold-formed steel joists developed serious flexural-

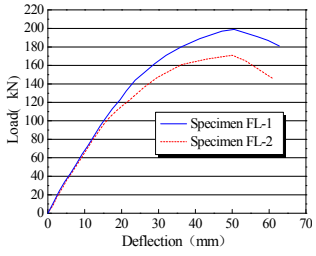

Figure 3 Load-deflection curves of specimens

torsional buckling (Figure 4). The load-deflection curves indicated that the screw spacing was the main factor to influence the flexural stiffness of the composite floor system at the elastic stage. When the load was increased to 105kN, the floor joists of the FL-2 developed flexural-torsional buckling； and at this point the load-deflection curves of FL-1and FL-2 started to go separate path. The screw spacing had sustained effects on the flexural capacity and stiffness when the floor systems were in plastic stage. The results showed when the screw spacing was increased from 150mm/300mm to 300mm/600mm, the maximum bearing capacity was declined 14.32%.

(a) web local buckling (b) OSB failure character (c) steel skeleton's failure of FL–2

Figure 4 Failure characteristics of composite floor

The floor specimens FL-1 and FL-2 had similar failure characteristics. When the load was small, the deflection at every loading step was steadily increased. With the increase of the load, the joists gradually developed web local buckling and the wave length was equal to the screw spacing between the joists and floor diaphragm (Figure 4(a)). During the whole experiment, the OSB sheathing did not exhibit noticeable bending deformation and tearing failure(Figure 4(b)). After the experiment, the OSB sheathing was dismantled, cold-formed steel joists occurred distortional buckling deformation and bending failure(Figure 4(c)). The deformation of FL-2 was more remarkable than that of FL-1.

3. Nonlinear finite element analysis of floor

3.1 Finite element model

The commercial software ANSYS was used to simulate the tested specimen. In finite element method, shell181 element was used to simulate cold-formed joists, tracks, bearing stiffeners and OSB sheathing. In addition, beam188 element was used to simulate self-drilling screw connections between the joists and OSB sheathing; the self-drilling self-tapping screws used in the steel skeleton were coupled. Meanwhile, 3D contact element-CONTAC52 was used between the joists and tracks, the joists and bearing stiffener; and the coefficient of friction

was taken as 0.3(Figure 5(a)). Mapped mesh method was adopted to mesh the geometry model, which had regular shape. Finite element model's boundary conditions and load were applied as shown in Figure 5(b): displacements along x, y, and z directions at the left support, and x and y directions at the right support were constrained. Line loads were applied at the locations where distribution beams were arranged.

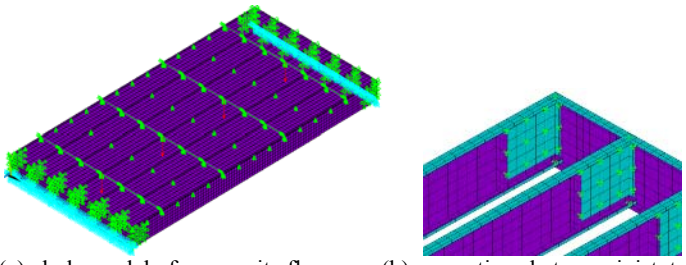

(a)whole model of composite floor (b)connections between joist, track and bearing stiffener

Figure 5 FEM model of floor

Table 1 Material behavior of OSB sheathing

	Bending elastic modulus /MPa	Flexure strength /MPa	Shear modulus /MPa	Shear strength /MPa	Poisson's ratio
Parallel to the longitudinal axis	5250	21.20	1180	8.2	0.30
Vertical to the longitudinal axis	1910	7.86	1280	7.9	0.11

Table 2 Comparisons of finite element analysis and test results of specimens

Specimen	P_u/kN From tests	P^*_u /kN From FEM analysis	P^*_u/P_u	Δ_u /mm From tests	Δ^*_u /mm From FEM analysis	Δ^*_u/Δ_u
FL-1	198.6	206.45	1.04	50.7	47.43	0.94
FL-2	170.16	182.12	1.07	50.22	48.33	0.96

Note: P_u is the ultimate bearing capacity from tests; Δ_u is the deflection corresponding to P_u;

P_u^* is the ultimate bearing capacity from FEM analysis;Δ^*_u is the deflection corresponding to P_u^*

Constitutive relation of cold-formed steel used in FEM was determined based on test results. The OSB sheathing was assumed isotropic. According to Thomas W.H.(2002) and the Chinese Standard LY/T 1580(2010), the mechanical property of 18mm thick OSB sheathing was listed in Table 1. Comparisons of FEM results and test results on flexural bearing capacity were listed in Table 2. Obviously FEM results agree well with the test results, which validated the finite element method used in this paper.

3.2 Finite Element Parametric Analyses

3.2.1 Influence of screw spacing on flexural capacity

Based on the finite element model of FL-1, a parameter study was carried out by changing the screw spacing and the size of cold-formed steel skeleton. The bearing capacities calculated was shown in Table 3.

Table 3 Influence of screw spacing to the bearing capacity of floor

Assembly description	Dimension of steel skeleton /mm	screw pacing /mm	P_u /kN
4.8m×2.4m (length×width); joists space 400mm; 18mm thick OSB; Material is same as FL–1	joist C305×41×14×1.6 track U305×35×1.6	300/300	196.68
		150/300	206.45
		100/300	210.38
		150/600	196.05
		150/300	206.45
		150/150	255.20
		150/100	269.81
	joist C255×41×14×1.6 track U255×35 ×1.6	300/300	164.31
		150/300	171.23
		100/300	175.21
		150/600	159.79
		150/300	171.44
		150/150	202.00
		150/100	215.55

Note：Screw spacing 150/300 was 150mm on-center at supported panel edges and 300mm on-center at intermediate supports.

From Table 3, it can be concluded that when reducing the screw spacing at diaphragm boundary edges from 300mm to 100mm while keeping the same screw spacing in the interior, the bearing capacity of the composite floor increased slightly. Therefore, the authors suggested the economical and reasonable screw spacing is 150mm on-center at OSB boundary edges. When keeping the same screws spacing at OSB boundary edges and gradually reducing the interior screw spacing from 600mm to 300mm, the bearing capacity of the composite floor was effectively improved. Furthermore the bearing capacity of the composite floor hardly changed when the interior screws spacing reduced from 300mm to 150mm, so the reasonable screw spacing is 50~300 mm on-center at intermediate supports.

3.2.2 Influence of length-width ratio on the flexural capacity

Based on the finite element model of FL-1, parameter analysis was carried out by changing the width of the floor system to simulate the influence of length-width ratio on the bearing capacity of composite floor. The results were shown in Table 4 and Figure 6. it is concluded that with the numbers of joists changed from 4 to 9, the bearing capacity of composite floor increased approximately linearly.

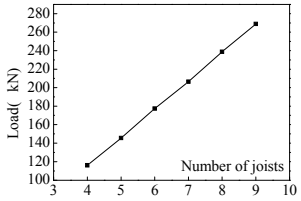

Figure 6 Influence of joists number on the bearing capacity of floor

Table 4 Influence of length-width ratio on the bearing capacity of floor

Assembly description /mm	Length×width /m	Length-width ratio	Number of joists	P_u /kN
Joist C305×41×14×1.6 Space 400; Track U305×35×1.6; 18 thick OSB; Screws spacing 150/300; Material property same FL–1	4.8×1.2	4	4	116.05
	4.8×1.6	3	5	145.51
	4.8×2.0	2.4	6	177.36
	4.8×2.4	2	7	206.45
	4.8×2.8	1.72	8	238.77
	4.8×3.2	1.5	9	268.75

4. Simplified design method to calculate the bearing capacity of floor

As shown in Figure 3, the specimens could continue to carry load after elsatic stage, but the deflection of the floor system increased rapidly with the development of buckling deformation. Plastic deformation affected the serviceability of the structures; therefore the yield flexural load was defined as the design bearing capacity of the composite floor system. Because of the impact of plate group effects, post-buckling related effects and other factors, the buckling stress of the joists was very complex, and the theoretical calculation of its yield bending moment was relatively difficult. Therefore, it is necessary to establish a simplified method to calculate the flexural bearing capacity of the composite floor system.

Based on the FEM analysis results in 3.2, the floor system can be simplified as T-shape composite beams and inverted L-shape composite beams to calculate its flexural bearing capacity. The equivalent diagram model was shown in Figure 7.

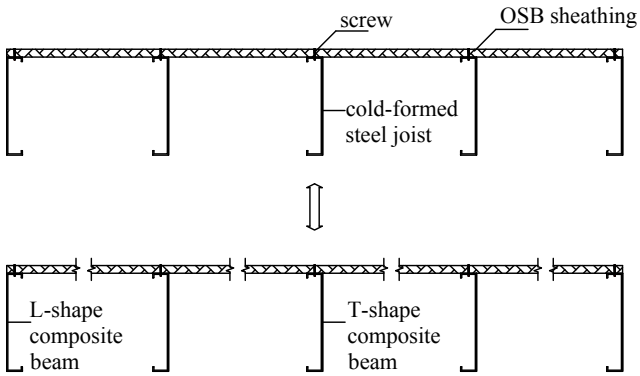

Figure7 Simplified model of composite floor

The yield moment of T-shape and L-shape cross section can be calculated through multiplying the joists' effective elastic flexural moment and a combination effect coefficient η .As shown in formula (1),

$$M_{\mathrm{y}} = \eta \cdot M_{\mathrm{cy}} \tag{1}$$

Where, M_y is the yield bending moment of the composite beam, which is the load when the joists' compression flange developed local buckling; M_{cy} is the effective elastic flexural moment of single joist, $M_{\mathrm{cy}} = W_{\mathrm{c}} \cdot f_{\mathrm{y}}$, W_{c} is the effective flexural resistance moment of single joist, f_{y} is the steel yield strength and η is the combined effect coefficient.

4.1 Establishment of the simplified model

A simplified FEM model was built as same as the overall FEM model in 3.1. The bearing capacity of T-shape and L-shape composite beams were shown in Table 5. Table 5 showed that the deference of the ultimate bearing capacity between the overall model and simplified model was within 5%, and the failure characteristics was similar (Figure 8), which validated the feasibility of calculating the floor's bearing capacity by the simplified method.

Table5 Bearing capacity of simplified composite beam and overall composite floor

Sample profiles /mm	Length ×width /m	Joist space /mm	Number of T-shape beam n_1	Number of L-shape beam n_2	$P_{u\text{-}T}$ /kN	$P_{u\text{-}L}$ /kN	$P_{u\text{-}J}$ /kN	P_u /kN	Error /%
Joist C305×41×14×1.6; Track U305×35×1.6; 18 OSB Screws spacing 150/150; Material is same as FL–1	4.8×2.0	400	4	2	41.44	32.01	229.78	239.76	4.34
	4.8×2.4	400	5	2			271.22	268.52	0.99
	4.8×2.8	400	6	2			312.66	309.34	1.06
	4.8×2.4	600	3	2	48.01	37.4	220.14	212.42	3.51
	4.8×3.0	600	4	2			268.58	257.50	4.12
	4.8×3.6	600	5	2			317.02	301.65	4.84

Note： $P_{u\text{-}T}$ is the ultimate bearing capacity of single T-shaped model;

$P_{u\text{-}L}$ is the ultimate bearing capacity of single pour L-shaped model;

$P_{u\text{-}J}$ is the ultimate bearing capacity of simplified model, $P_{u\text{-}J} = n_1 P_{u\text{-}T} + n_2 P_{u\text{-}L}$;

P_u is the ultimate bearing capacity of overall floor by FEM analysis.

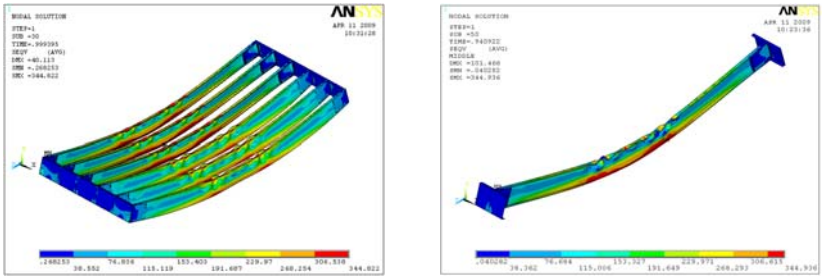

(a)failure characteristics of overall floor (b)failure characteristics of simplified T-shape beam

Figure 8 Comparison of failure character between the overall floor and T-shape beam

4.2 Determination of combination effect coefficient η

4.2.1 Influence of joist thickness on the coefficient η

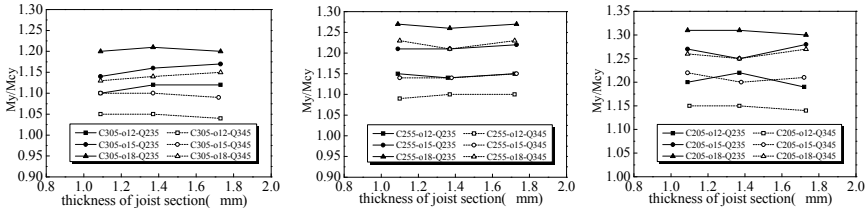

(a)C305 specimens (b)C255 specimens (c)C205 specimens

Figure 9 Influence of thickness of joist section on coefficient η

As shown in Figure 9, the effect of thickness of joist section on the coefficient η was investigated by selecting a T-shape composite beam: the beam span was 4.8m with 400mm wide OSB sheathing, and the screw spacing was 150mm. In the analysis, the material properties, web height of joist and thickness of OSB were changed. Figure 9 indicated that the increase of the joist section thickness have no obvious effect on coefficient η and can be ignored in simplified model.

4.2.2 Influence of OSB thickness on coefficient η

The effect of OSB thickness on the coefficient η was analyzed by using of a T-shape composite beam: the beam span was 4.8m with 400mm wide OSB sheathing, and the screw spacing was 150mm. In the analysis, the material property and web height of joist and thickness of OSB were changed.

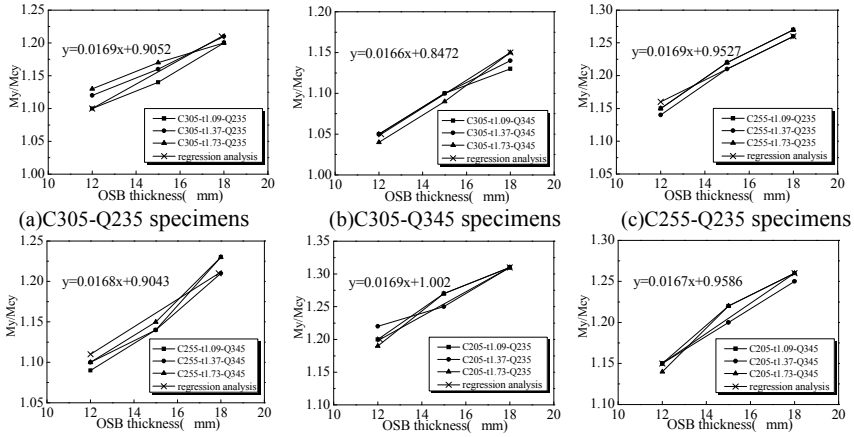

(a)C305-Q235 specimens (b)C305-Q345 specimens (c)C255-Q235 specimens

(d)C255-Q345 specimens (e)C205-Q235 specimens (f)C205-Q345 specimens

Figure 10 Influence on η due to change in thickness of OSB sheathing

Table 6 Coefficient c vs. steel yield strength and web height of joist

Joist \ Steel	Q235	Q345
C205×41×14×1.6	1.002	0.959
C255×41×14×1.6	0.953	0.904
C305×41×14×1.6	0.905	0.847

As shown in Figure 10, with the increase of OSB thickness, the coefficient η increased gradually and approximately linearly. Independent regression analysis results of coefficient η were also shown in Figure 10. Based on the regression, coefficient η can be expressed approximately as $\eta = 0.0168t_c + c$, where c is related to steel yield strength and web height of the joist, as shown in Table 6.

4.2.3 Influence of screw spacing on coefficient η

The effect of screw spacing on the coefficient η was analyzed by employing a T-shape composite beam: the beam span was 4.8m with 400mm wide OSB sheathing, and the screw spacing was varied from 150mm to 300mm. In the analysis, the material property and web height of joist were changed. The calculation results were shown in Table 7. When the inside screw spacing was changed from 150mm to 300mm, the coefficient η could be approximately expressed as $\eta_{T-300} \approx 0.85\eta_{T-150}$.

Table 7 Influence of screw spacing on η

Joist dimension /mm	Steel	Thickness of OSB /mm	η_{T-150}	η_{T-300}	$\frac{M_{y\text{-}300}}{M_{y\text{-}150}}$
C305×41×14×1.73	Q235	12	1.081	0.952	0.881
		15	1.125	0.986	0.877
		18	1.158	1.014	0.875
	Q345	12	1.005	0.853	0.849
		15	1.049	0.885	0.844
		18	1.108	0.938	0.846
C255×41×14×1.73	Q235	12	1.102	0.976	0.886
		15	1.169	1.017	0.870
		18	1.218	1.075	0.883
	Q345	12	1.056	0.914	0.866
		15	1.102	0.935	0.848
		18	1.184	1.010	0.853

4.2.4 Influence of joist spacing on coefficient η

The effect of joist spacing on the coefficient η was analyzed by employing a T-shape composite beam: the beam span was 4.8m with 600mm wide OSB sheathing, and the screw spacing was 150mm. In the analysis, the web height of joist and the thickness of OSB were changed. The calculation results (shown in Table 8) indicated that when the joist spacing was changed from 400mm to 600mm, the coefficient η can be approximately expressed as $\eta_{\mathrm{T600-150}} \approx 1.09\eta_{\mathrm{T400-150}}$.

Table 8 Influence of joist spacing on η

Joist dimension /mm	Steel	Thickness of OSB /mm	$\eta_{\mathrm{T400-150}}$	$\eta_{\mathrm{T600-150}}$	$\frac{\eta_{\mathrm{T600-150}}}{\eta_{\mathrm{T400-150}}}$
C305×41×14×1.73	Q235	12	1.186	1.299	1.096
		15	1.251	1.367	1.092
		18	1.286	1.428	1.110
	Q345	12	1.005	1.091	1.086
		15	1.049	1.160	1.106
		18	1.108	1.216	1.097
C255×41×14×1.73	Q235	12	1.240	1.365	1.101
		15	1.280	1.420	1.110
		18	1.360	1.466	1.078
	Q345	12	1.056	1.162	1.100
		15	1.102	1.249	1.134
		18	1.184	1.309	1.106

4.2.5 Influence of inverted L-shape composite beam on coefficient η

The inverted L-shape composite beam was established to study the influence on coefficient η. In the analysis, the material property, web height of joist and the thickness of OSB were changed. The calculation results (shown in Table 9) indicated that coefficient η could be approximately expressed as $\eta_{\mathrm{L400\text{-}150}} = (0.85 \sim 0.90)\eta_{\mathrm{T400\text{-}150}}$.

In summary, the combination coefficient η could be calculated as

$$\eta = \alpha \cdot \beta \cdot (0.0168t_c + c) \qquad (2)$$

Where α is the influence coefficient for the joists spacing; when joists spacing is 400mm, $\alpha = 1$; when joists spacing is 600mm, $\alpha = 1.09$. t_c is the thickness of OSB, mm. β is the influence coefficient for the screw spacing; when screw spacing is 150/150mm, $\beta = 1$; when screw spacing is 150/300mm, $\beta = 0.85$. c is a coefficient shown in Table 6.

Table 9 Influence on η due to change in cross-section of simplified model

Joist dimension /mm	Steel	Thickness of OSB /mm	$\eta_{\text{T400-150}}$	$\eta_{\text{L400-150}}$	$\frac{\eta_{\text{L400-150}}}{\eta_{\text{T400-150}}}$
C305×41×14×1.73	Q235	12	1.081	0.966	0.894
		15	1.125	1.005	0.893
		18	1.158	1.037	0.895
	Q345	12	1.005	0.883	0.879
		15	1.049	0.928	0.884
		18	1.108	0.932	0.859
C255×41×14×1.73	Q235	12	1.102	0.991	0.898
		15	1.169	0.998	0.853
		18	1.218	1.066	0.875
	Q345	12	1.056	0.950	0.900
		15	1.102	0.987	0.896
		18	1.184	1.022	0.864

In order to validate the regression equations, the ultimate load-bearing capacity of 6 composite floor systems were calculated by Eq. 1 and Eq. 2. The comparison of the flexural bearing capacity from simplified method and FEM analysis were listed and compared in Table 10. Table 10 showed the bearing capacities calculated by above equations agreed well with those from FEM analysis, which verified that it was simple and feasible to calculate the ultimate flexural bearing capacity of the floor systems by the suggested Eq. 1 and Eq.2.

Table 10 Comparison of bearing capacity from simplified method and FEM analysis

Sample profiles /mm	Joist dimension /mm	Thickness of OSB /mm	$M_{\text{y-S}}$	$M_{\text{y-FEA}}$	$\frac{M_{\text{y-S}}}{M_{\text{y-FEA}}}$
Joists spacing 400; Q235; Screws spacing 150/300	C205×41×14×1.6	16	6.96	7.78	0.895
	C255×41×14×1.6	14	8.94	9.86	0.906
	C305×41×14×1.4	14	9.87	10.25	0.963
Joists spacing 600; Q345; Screws spacing 150/300	C205×41×14×1.6	16	10.75	11.66	0.922
	C255×41×14×1.6	14	13.72	13.75	0.998
	C305×41×14×1.4	14	14.98	14.86	1.009

Note： $M_{\text{y-S}}$ is the bearing capacity from simplified method；

$M_{\text{y-FEA}}$ is the bearing capacity from FEM analysis.

5. Conclusion

In this paper, two full scale specimens are tested to study the flexural capacity of cold-formed steel joists and OSB composite floor systems, and at the same time an experimental validated finite element method is established. Then extensive parameter analyses are carried out by finite element method. Finally, based on results from parameter analyses, a simplified method for calculating the ultimate load-bearing capacity of the floor system is proposed. From above analysis, the following conclusions can be obtained:

(1).The cold-formed steel joists and OSB composite floors have high bearing capacity and small deformation. The main failure characteristics are flexural-torsional buckling of the floor joists. The screw spacing significantly affects the load-carrying capacity but has little effects on the elastic stiffness of composite floor systems.

(2).Through extensive FEM parameter analyses, the reasonable screw center spacing is suggested as 150mm at OSB edges and 150~300mm at intermediate supports. The load-carrying capacity of the composite floor systems linearly increases as the number of joists increase. The flexural capacity of the composite floor systems can be calculated by simplifying it to a T-shape composite beam.

Acknowledgments

The authors are grateful for the financial support provided by National Natural Science Foundation of China (No.51108033) and Central University Basic Research Foundation (CHD2013G3286001).

References

GB/T 228.1(2010). Metallic materials–tensile testing at ambient temperature. Beijing: China Standard Press, 2010(in Chinese).

GB 50018(2002).Technical code of cold-formed thin-wall steel structures.Beijing: Standards Press of China,2002(in Chinese) .

LY/T 1580(2010). Oriented strand board. Beijing: China Standard Press,2010(in Chinese).

Nader R., Elhajj P.E., et al.(1999). Innovative residential floor construction: horizontal diaphragm values for cold–formed steel framing. NAHB Research Center, United states.

North American Steel Framing Alliance(2000). Prescriptive method for residential cold-formed steel framing. Prepared by the NAHB Research Center, Inc., for the American Iron and Steel Institute, the U.S. Department of Housing and Urban Development and the National Association of Home Builders. Upper Marlboro, MD.

Teng X.F., Cao B.Z., Xu Chao, et al.(2009). Experimental research on cold formed steel–OSB floor. Journal of Jilin Institute of Architecture & Civil Engineering, 26(2):1-5(in Chinese).

Thomas W.H.(2002). Concentrated load capacity and stiffness of oriented strand board: calculation versus test. Journal of Structural Engineering, 128(7):908-912.

Xu L., Tangorra F.M.(2007). Experimental investigation of lightweight residential floors supported by cold-formed steel C-shape joists.Journal of Constructional Steel Research, 63:422-435.

Xu L.(2011). Floor Vibration in Lightweight Cold–Formed Steel Framing. Advances in Structural Engineering, 14(4):659-672.

Zhou X.H., Jia Z.W.(2010). Experimental study on flexural capacity of cold-formed steel joists and concrete composite floor. Journal of Building Structures, 31(7): 13-22(in Chinese).

Zhou X.H., Li Z., Wang R.C. et al. (2013).Study on load–carrying capacity of the cold-formed steel joists–OSB composite floor. China Civil Engineering Journal, 46(9):1-11(in Chinese).